ON THE OBSERVED RESULTS OF THE INTENSITY AND THE POLARIZATION OF NARROW-BAND AURORAL HISS EMISSIONS

Masanori NISHINO, Yoshihito TANAKA, Akira IWAI, Tetsuo KAMADA

Research Institute of Atmospherics, Nagoya University, 13, Honohara 3-chome, Toyokawa 442

and

Takeo HIRASAWA

National Institute of Polar Research, 9–10, Kaga 1-chome, Itabashi-ku, Tokyo 173

Abstract: Results of intensity and polarization measurements of narrow-band auroral hiss observed simultaneously with the direction finding (DF) observations at Syowa Station, Antarctica, are compared with results of the full-wave calculation in a realistic ionospheric model. The ratios of the 8 kHz hiss intensity observed at Syowa to that at Mizuho Station (about 270 km distant from Syowa in the geomagnetic south direction) depend on the propagation distance from the exit regions at the height of the lower edge of the ionosphere to the two ground stations. However, the observed ratios (SY/MI) are 2–3 dB higher than the corresponding theoretical values. The disagreement is discussed as regards to the effects of the wave polarization and the ground conductivity at the observing site on the received wave intensity.

The distribution of R/L (R- to L-handed polarized component) values of the narrow-band auroral hiss observed at Syowa with incident angles indicates a similar tendency to the R/L values for the limiting polarization by full-wave calculation, but the observed values are smaller than the calculated ones. The disagreement seems to be caused by the low accuracy of DF at small incident angles, and by the disturbance from strong VLF atmospherics.

1. Introduction

It has been found that continuous hiss emissions with a narrow frequency band ($\lesssim$20 kHz) are usually observed in association with auroral arcs appearing in the geomagnetic south of Syowa Station (geomag. lat. $-70.4°$), Antarctica (MAKITA and FUKUNISHI, 1973; MAKITA, 1979). The authors have developed a new direction finding (DF) system of auroral hiss at Syowa in 1978, based on the measurement of the arrival time difference among three spaced points, in order to study the propagation mechanism of auroral hiss in the ionosphere and the magnetosphere (NISHINO *et al.*, 1981). From the comparison between the DF results of auroral VLF hiss and the all-sky photographs of aurora, we (NISHINO *et al.*, 1982) have indicated that the exit region of the narrow-band hiss at the lower ionosphere is located at lower latitudes side of the location of aurora which appeared from the zenith to the geomagnetic south of Mizuho Station

(geomag. lat. −72.3°). This observational result suggests that the narrow-band hiss emissions propagate downwards from the upper ionosphere in a nonducted mode, deviating from the field-aligned duct, as proposed from the ray-path computation by SRIVASTAVA (1974), SINGH and SINGH (1978) and MAKITA (1979). The hiss emissions whose wave normal is within the transmission cone at the height of F region penetrate through the ionosphere and escape from the exit region at the lower edge of the ionosphere, and thereafter the emissions reach the ground.

In order to improve our understanding of the propagation mechanism of auroral hiss, we first describe in this paper the intensity and polarization of VLF hiss measured simultaneously with the DF observations of auroral VLF hiss. Next, we compare the observed results with the theoretical ones obtained by means of the full-wave calculation (PITTEWAY and JESPERSEN, 1966) in a realistic model of the auroral ionosphere, and discuss the difference between them.

2. Observed Results

2.1. *Hiss intensity*

Figure 1 shows an example of the temporal variation of 8 kHz hiss intensities observed at Syowa and Mizuho (Fig. 1a), and the arrival directions of auroral VLF hiss (5–8 kHz) and the location of aurora sketched by all-sky photograph observed at Syowa (Fig. 1b). Auroral hiss emissions are received at the both stations by the

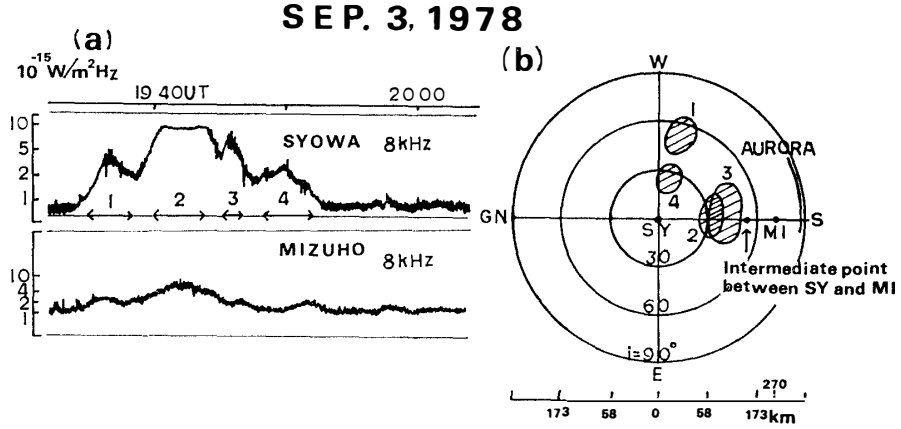

Fig. 1. An example of the temporal variation of 8 kHz hiss intensities observed at Syowa and Mizuho Stations (a), and the arrival directions of auroral VLF hiss (5–8 kHz) and the aurora sketched by all-sky photograph observed at Syowa (b).

loop antennas whose planes are oriented in the geomagnetic N-S direction. The hiss event shown in Fig. 1 is divided into four sub-events. The exit regions of sub-events 1 and 4 are located to the geomagnetic west of Syowa, and those of sub-events 2 and 3 are located to the geomagnetic south of Syowa. The exit regions of hiss emissions are assumed to be at 100 km in the lower ionosphere. As can be seen from the figure the exit regions of all sub-events are located nearer to Syowa than to Mizuho, and it can be expected that the hiss intensity at Syowa is higher than that at Mizuho.

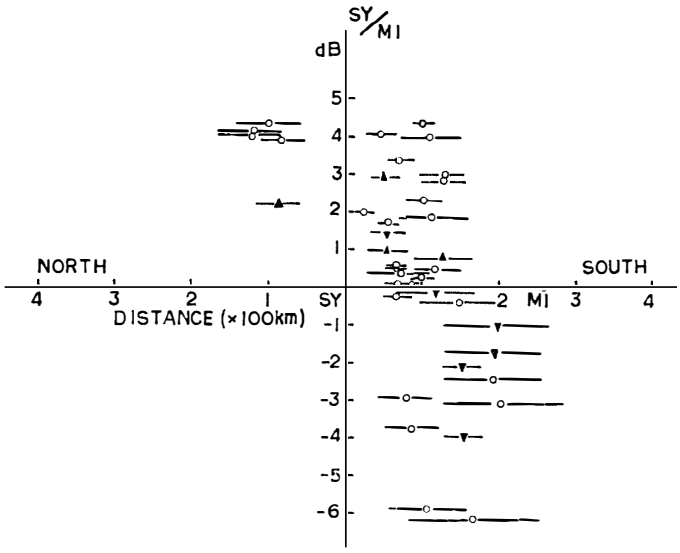

Fig. 2. Relation between the position of the exit regions of the narrow-band hiss propagated approximately along the geomagnetic meridian plane and the intensity ratio (SY/MI) of 8 kHz hiss observed at Syowa to that at Mizuho. Horizontal bars indicate the spread of the exit regions, and the mark (○) at the center of the bar represents the ratio estimated normally, the mark (▲) represents the case in which the record at Syowa was saturated at 8 kHz, and the mark (▼) represents the case in which the one at Mizuho was saturated.

Figure 2 shows the relation between the position of the exit regions of the narrow-band hiss propagated approximately along the geomagnetic meridian plane and the intensity ratio (SY/MI) of 8 kHz hiss observed at Syowa to that at Mizuho. Horizontal bars indicate the spread of the exit regions, and the mark (○) at the center of the bar represents the ratio estimated normally, the mark (▲) represents the case in which the record at Syowa was saturated at 8 kHz, and the mark (▼) represents the case in which the one at Mizuho was saturated. The intensity ratios in dB show always plus when the exit region was north of Syowa, but they scatter widely plus and minus when the exit region was within 100 km south of Syowa. This scattering may be due to the reduction of DF accuracy when incident angle is small. Disregarding this scattering we may conclude that the intensity ratios decrease from the north of Syowa towards the south. This result indicates that the intensity of narrow-band hiss on the ground depends on the propagation distance from the exit to the ground station.

In order to evaluate these observed results, we have carried out the full-wave calculations of the penetration of VLF waves through the ionosphere. Figure 3 shows the ionospheric model used for the calculations. The electron density profile with height is derived from the statistical analysis of the data observed on board the rockets launched at Syowa at the time of appearance of aurora (HIRASAWA and YAMAGISHI, 1979). Since most of hiss events analyzed in this paper are obtained during a relatively quiet aurora, we took 1 kR curve of auroral luminosity in this figure. The collision frequency profile is derived from being proportional to the atmospheric pressure (THRANE and PIGGOTS, 1966). The calculations are made in the case of the dip angle of $-65.46°$ and the gyrofrequency of 1592.85 kHz at Syowa for the true geomagnetic field (IRGF 75).

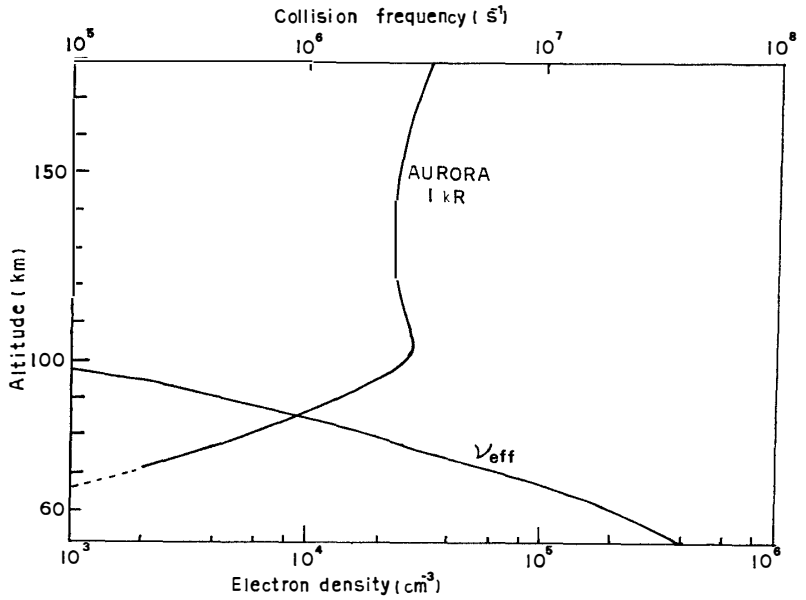

Fig. 3. Ionospheric model used for the full-wave calculation. Auroral luminosity of 1 kR corresponds to a relatively quiet aurora.

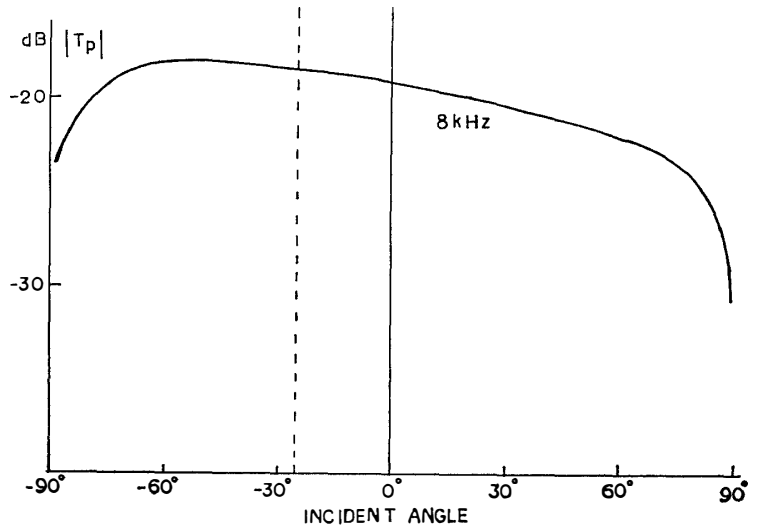

Fig. 4. Variation of the transmission coefficients (in dB) of downgoing VLF waves at 8 kHz with incident angles.

Figure 4 shows the variation of the transmission coefficients (in dB) of downgoing VLF waves of 8 kHz with incident angles. A vertical dotted line indicates the incident angle parallel to the earth's magnetic field intersecting Syowa. The ratios of received intensities at Syowa to those at Mizuho as regards to the exit position are estimated by using these transmission coefficients, and they are illustrated by the solid curve in Fig. 5. The tendency of gradual decrease of ratio from the north of Syowa towards Mizuho coincides with the observed results in Fig. 2, but the observed ratios are 2–3 dB higher on the average than the calculated ratio.

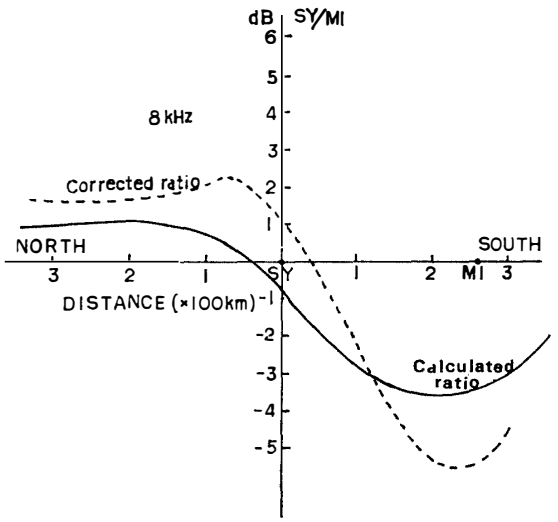

Fig. 5. Ratios of received intensities at Syowa to those at Mizuho as regards to the position of exit estimated by using the transmission coefficient of Fig. 4 (solid curve). Broken curve shows the intensity ratio corrected by the effects of the wave polarization and the ground conductivity at the observing site (see Discussion).

2.2. *Polarization*

Figure 6 shows an example of the temporal variation of the polarization at 8 kHz auroral hiss observed at Syowa. A crossed loop antenna with the planes oriented in N-S and E-W directions is used for the measurement of polarization. It is found from this figure that the narrow-band hiss comes to Syowa with right-handed elliptically polarization. Figure 7 shows the distribution of the ratio R/L (R- to L-handed polarized component) of the narrow-band hiss observed at Syowa in 1978, as a function of incident angles. Most of the ratios are distributed less than about 2.5. It seems that the ratios slightly increase with decreasing incident angles for the hiss emissions coming from the south of Syowa. In order to evaluate these observed results, we calculate the limiting polarization of VLF waves penetrating through the ionosphere by means of the full-wave calculations.

Figure 8 shows the limiting polarization with which the downgoing waves emerge into free space below the ionosphere. The model used in the calculations is shown in Fig. 3. The variation of ψ indicating the modulus of the polarization ellipse projected on the ground, is about 45° around the incident angle of 0°. The variation of ψ, indicating the argument is about 90° within the incident angles of $\pm 30°$, that is, the polarization is nearly right-handed circular at small incident angles. By the use of the

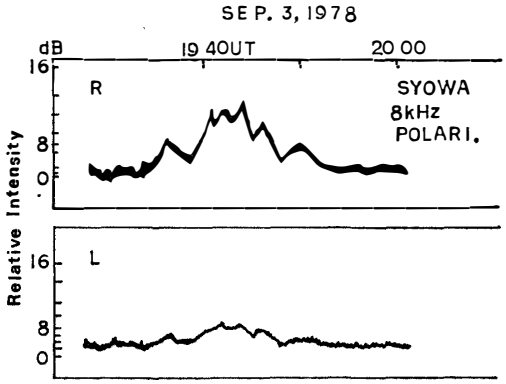

Fig. 6. An example of the temporal variation of the polarization at 8 kHz auroral hiss observed at Syowa.

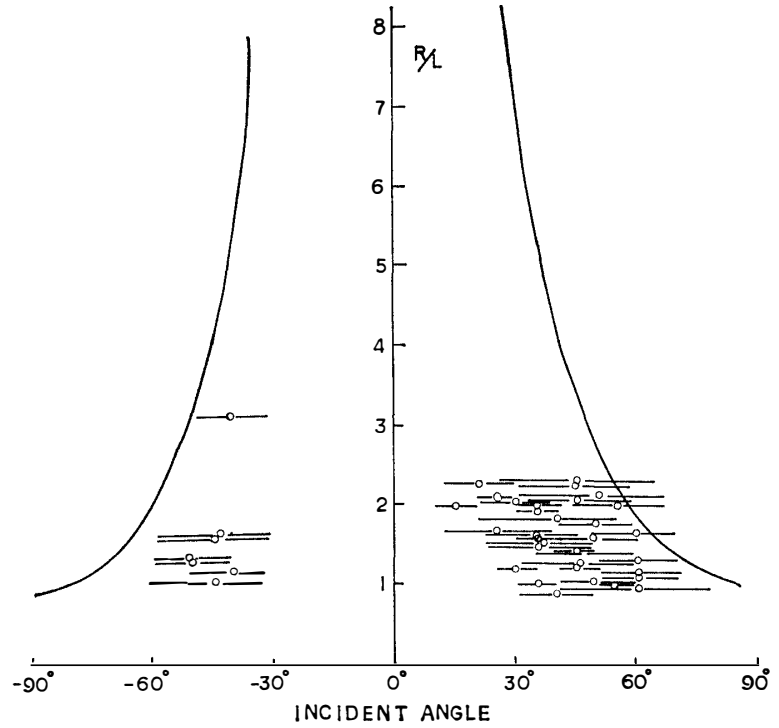

Fig. 7. Distribution of the ratio R/L (R- to L-handed polarized component) of the narrow-band hiss observed at Syowa in 1978, as a function of incident angles. Two solid curves show the calculated ratios obtained by the limiting polarization shown in Fig. 8.

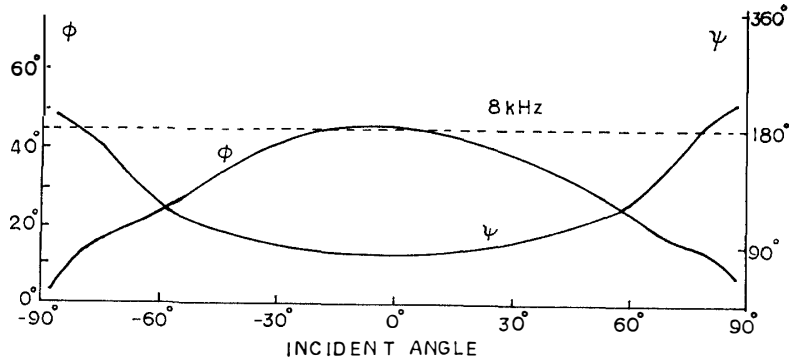

Fig. 8. Limiting polarization with which the downgoing waves emerge into free space below the ionosphere caluculated by the use of the ionospheric model of Fig. 3.

values of ϕ and ψ, the ratio (R/L) are calculated by the following equation,

$$R/L=\left[\frac{k^2+1-2k\sin\psi}{k^2+1+2k\sin\psi}\right]^{1/2}, \tag{1}$$

where $k=\tan\phi$.

The calculated ratios are represented by the two solid curves shown in Fig. 7. The tendency showing the increasing ratio with decreasing incident angles coincides with that of the observed results shown by the horizontal bars in Fig. 7, but the observed ratios are smaller than the calculated ratios at all incident angles.

3. Discussion

As shown in Figs. 2 and 5, the intensity ratio (SY/MI) of 8 kHz hiss observed at Syowa to that at Mizuho indicates the similar tendency to the ratio estimated from the variation of transmission coefficients obtained by the full-wave calculation, but the observed ratios are higher by 2–3 dB than the calculated values. Let us discuss the effects of the wave polarization and of different ground reflections at the two stations on the intensity ratio.

We choose the narrow-band hiss propagated along the meridian plane, and describe the intensities received by the loop antennas whose planes are oriented in the geomagnetic N-S direction. Figure 9 shows the configuration of the electromagnetic fields at receiving point P in the geomagnetic N-S plane. Then, the magnetic field induced in the x-direction is given by only the component of TM mode.

$$H_x = -(1+{}_{\parallel}R_{\parallel}e^{-j\frac{4\pi h}{\lambda}\cos i})H_1$$
$$\simeq -(1+{}_{\parallel}R_{\parallel})H_1 \quad (h \ll \lambda)\,, \tag{2}$$

where

i : incident angle,
H_1 : magnetic field of TM mode wave,
${}_{\parallel}R_{\parallel}$: ground reflection coefficient of TM mode wave,
λ : wavelength,
h : height of the receiving point P.

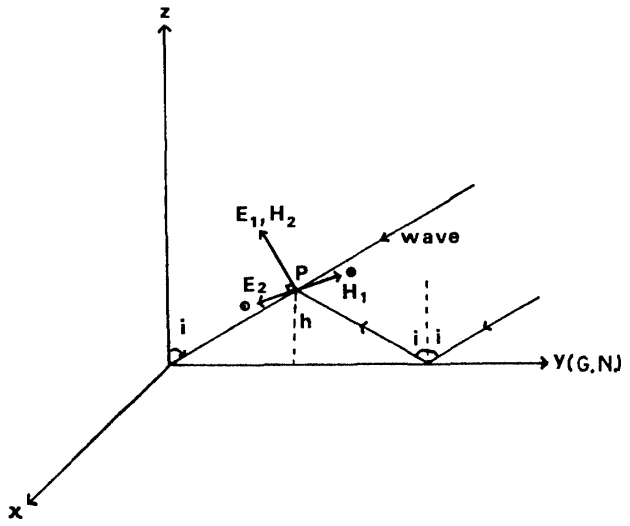

Fig. 9. Electromagnetic fields at the receiving point P in the geomagnetic meridian plane. E_1 and H_1 correspond to TM mode wave, while E_2 and H_2 to TE mode wave.

The field intensity is affected by the ground reflection coefficient in form of $G_{\mathrm{eff}} = 1+{}_{\parallel}R_{\parallel}$. Since the ground is assumed to be rock at Syowa, while that is assumed to be ice at Mizuho, the field intensity is different between the two stations even if the incident wave intensities are the same at the both stations.

As shown in the calculated result of the limiting polarization of Fig. 8, vertically

downgoing waves emerging into free space indicate nearly circular polarization, while obliquely downgoing waves indicate elliptic polarization. Therefore, it is required that the magnetic field intensity receiving the wave energy with elliptic polarization is modified as the reference to the wave energy with circular polarization. It is assumed that the magnetic fields at point P in Fig. 9 are given by a monochromatic sine wave as follows;

$$H_1 = N \sin \omega t \,, \tag{3}$$

$$H_2 = A \sin (\omega t + \alpha) \,. \tag{4}$$

N and A are the amplitude of the magnetic fields of TM and TE mode waves, respectively, and α is the phase difference between the TM and TE mode waves. The average value of the Poynting vector (wave energy) of the direct sky wave is given as follows (BUDDEN, 1961);

$$\begin{aligned} \bar{\Pi} &= 1/2R(\boldsymbol{E} \times \boldsymbol{H}^*) \\ &= 1/2(N^2 + A^2) \,, \end{aligned} \tag{5}$$

where R denotes the real part, and star $*$ complex conjugate. Then, the wave energy ratio stored in H_1 to the total energy is $N^2/(N^2+A^2)$, that is, the amplitude ratio corresponds to $1/\sqrt{1+(A/N)^2}$. In the case of incident wave with circular polarization, the amplitude ratio is $1/\sqrt{2}$. Accordingly, the modification factor (P_{eff}) for elliptically polarization wave is given by the polarization ratio (A/N) as the reference to the wave with circular polarization.

$$P_{\mathrm{eff}} = \frac{\sqrt{2}}{\sqrt{1+(A/N)^2}} \,.$$

Table 1. Calculated modification factors of P_{eff} and G_{eff}, and the modified intensity ratios in dB.

Incident angle		Syowa		Mizuho		Modified ratio (in dB)
SY	MI	P_{eff}	G_{eff}	P_{eff}	G_{eff}	
−80	−83	1.173	1.387	1.198	1.350	0.052
−70	−80	0.972	1.647	1.173	1.270	0.625
−60	−77	0.935	1.749	1.095	1.380	0.686
−50	−76	0.967	1.801	1.075	1.420	1.145
−40	−74	0.992	1.831	1.025	1.460	1.682
−30	−73	1.007	1.850	1.005	1.480	1.955
−20	−72	1.013	1.861	0.995	1.550	2.029
−10	−71	1.013	1.867	0.980	1.530	2.017
0	−70	1.007	1.869	0.972	1.550	1.933
10	−68	0.995	1.867	0.955	1.570	1.861
20	−66	0.978	1.861	0.950	1.600	1.565
30	−64	0.954	1.850	0.940	1.610	1.335
40	−62	0.933	1.831	0.935	1.640	0.845
50	−56	0.883	1.801	0.945	1.690	−0.037
60	−44	0.847	1.749	0.980	1.750	−1.272
70	0	0.909	1.647	1.007	1.818	−1.747
80	71	1.157	1.387	0.920	1.530	1.139

Table 1 shows the calculated modification factors, G_{eff} and P_{eff}, and the modified intensity in dB. The corresponding incident angles at Mizuho to those at Syowa are calculated by assuming the height of wave exit point is 100 km and the distance between the two stations is 270 km. The intensity ratio corrected by the method mentioned above is shown by the broken curve in Fig. 5. It is recognized that the corrected curve approaches to the observation result.

As shown in Fig. 7, the observed ratio (R/L) of the wave polarization is smaller than the calculated values at all incident angles. TANAKA *et al.* (1976) calculated the R/L values of waves with right-handed circular polarization from two and three directions, on which the phase of each wave is taken to be distributed completely at random. Their calculated results indicate the possibility of the occurrence probability of the R/L values less than 3. Therefore, the disagreement between calculations and observations may be due to the sum of a few wave packets propagated from a few of localized exit regions. However, it seems that practical difficulty in estimating accurately the R- and L-components of auroral hiss from the received signals superimposed by background atmospherics is another cause of observed small R/L values.

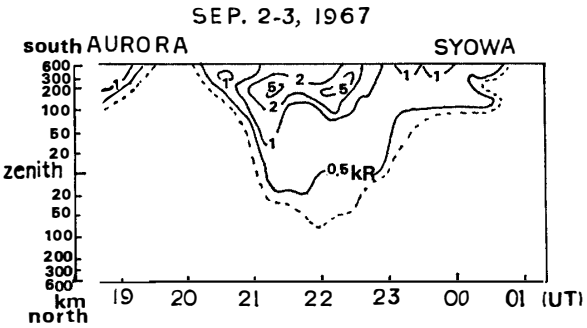

Fig. 10. An example of the meridian scanning photometer record of aurora, in which auroral display expands widely from high to low latitudes with decreasing luminosity (after HIRASAWA and NAGATA, 1972).

As shown in Fig. 1, the narrow-band hiss emissions are observed at Syowa, associated with the appearance of auroral arc in the south of Mizuho. We show an example of the meridian scanning photometer record of aurora in Fig. 10, in which auroral display expands widely from high to low latitudes with decreasing luminosity. Thus, the ionospheric model with the horizontal gradient of electron density in the lower ionosphere is important for the full-wave calculations.

Acknowledgments

The authors thank Prof. J. OHTSU and Dr. M. HAYAKAWA of the Research Institute of Atmospherics, Nagoya University for their valuable discussions. Two of the authors (M. N and T. H.) wish to express their gratitude to the kind cooperation given by the wintering members of the 19th Japanese Antarctic Research Expedition for the observations of VLF emissions and other geophysical phenomena at Syowa and Mizuho Stations.

References

BUDDEN, K. G. (1961): Radio Waves in the Ionosphere. Cambridge, Cambridge University Press, 11–23.

HIRASAWA, T. and NAGATA, T. (1972): Constitution of polar substorm and associated phenomena in the southern polar region. Mem. Natl Inst. Polar Res., Ser. A (Aernomy), **10**, 76 p.

HIRASAWA, T. and YAMAGISHI, H. (1979): Electron number density within auroras. Japanese IMS Program, Tokyo, Inst. Space Aeronaut. Sci., Univ. Tokyo, 27.

MAKITA, K. (1979): VLF-LF hiss emissions associated with aurora. Mem. Natl Inst. Polar Res., Ser. A (Aeronomy), **16**, 126 p.

MAKITA, K. and FUKUNISHI, H. (1973): Syowa Kiti ni okeru VLF emisshon kansoku (1970–1971), 1. Ôrorahisu to ôrora (Observation of VLF emissions at Syowa Station in 1970–1971, 1. Relationship between the occurrence of auroral hiss emissions and the location of auroral arcs). Nankyoku Shiryô (Antarct. Rec.), **45**, 1–15.

NISHINO, M., TANAKA, Y., IWAI, A. and HIRASAWA, T. (1981): A new direction finding technique for auroral VLF hiss based on the measurement of time difference of arrival at three spaced observing points. Planet. Space Sci., **29**, 365–375.

NISHINO, M., TANAKA, Y., IWAI, A., KAMADA, T. and HIRASAWA, T. (1982): Comparison between the arrival direction of auroral hiss and the location of aurora observed at Syowa Station. Mem. Natl Inst. Polar Res., Spec. Issue, **22**, 35–45.

PITTEWAY, M. L. V. and JESPERSEN, J. L. (1966): A numerical study of the excitation, internal reflection and limiting polarization of whistler waves in the lower ionosphere. J. Atmos. Terr. Phys., **28**, 17–43.

SINGH, D. P. and SINGH, B. (1978): Propagation characteristics of ground observed VLF waves after emerging from the ducts in the ionosphere. Ann. Geophys., **34**, 113–118.

SRIVASTAVA, R. N. (1974): Propagation of VLF emissions in the magnetosphere and in the ionosphere. Planet. Space Sci., **22**, 1545–1564.

TANAKA, Y., HAYAKAWA, M. and NISHINO, M. (1976): Study of auroral hiss observed at Syowa Station, Antarctica. Mem. Natl Inst. Polar Res., Ser. A (Aeronomy), **13**, 58 p.

THRANE, E. V. and PIGGOTT, W. R. (1966): The collision frequency in the *E*- and *D*-regions of the ionosphere. J. Atmos. Terr. Phys., **28**, 721–737.

(*Received April 30, 1982; Revised manuscript received January 5, 1983*)